Hall, S. J., Liptzin, D., Buss, H., DeAngelis, K., & Silver, W. L. (2016). Drivers and patterns of iron redox cycling from surface to bedrock in a deep tropical forest soil: a new conceptual model. *Biogeochemistry*, *130*(1), 177-190. https://doi.org/10.1007/s10533-016-0251-3

Drivers and patterns of iron redox cycling from surface to bedrock in a deep tropical forest soil: a new conceptual model

Steven J. Hall*[1], Daniel Liptzin[2], Heather L. Buss[3], Kristen DeAngelis[4], Whendee L. Silver[5]

[1]Department of Ecology, Evolution, and Organismal Biology, Iowa State University, 251 Bessey Hall, Ames, Iowa, 50011, USA

[2]INSTAAR, University of Colorado - Boulder, Boulder, CO, USA

[3]School of Earth Sciences, University of Bristol, Wills Memorial Building, Queens Road, Bristol BS8 1RJ, UK

[4]Department of Microbiology, University of Massachusetts Amherst, Amherst, Massachusetts USA

[5]Department of Environmental Science, Policy, and Management, University of California-Berkeley, Berkeley, California USA

* Corresponding author: stevenjh@iastate.edu, 515-294-7650

Key words: Critical zone, Iron oxidation, Iron reduction, Mineral weathering, Oxygen, Redox, TEAP

Abstract

Iron (Fe) reduction and oxidation are important biogeochemical processes coupled to decomposition, nutrient cycling, and mineral weathering, but factors controlling their rates and spatial distribution with depth are poorly understood in terrestrial soils. In aquatic ecosystems, Fe reduction often occurs below a zone of oxic sediments. We tested an alternative conceptual model for Fe redox cycling in terrestrial soils using a deep humid tropical forest soil profile. We hypothesized that Fe reduction in anaerobic microsites scales with depth variation in labile C and Fe availability, as opposed to bulk oxygen (O_2). We measured bulk O_2 at multiple depths from 0.1–5 m quasi-continuously over 18 months and sampled soils from surface to bedrock (~7 m). Median O_2 mixing ratios declined from 19.8 ± 1.2% at 0.25 m to 16.1 ± 1.0% at 1 m, but did not consistently decrease below 1 m, challenging a recent model of regolith development. Reduced Fe (Fe(II)) extractable in 0.5 M hydrochloric acid was greatest in 0 – 0.1 m soil and declined precipitously with depth, and did not correspond with visible gleying in B horizons. We observed similar depth trends in potential Fe reduction under anaerobic conditions. Depth trends in Fe(II) also closely mirrored short-term soil respiration and bulk soil C. Labile C stimulated Fe reduction at 0 – 0.1 m depth, whereas addition of short-range-ordered Fe oxides had no effect. Cultivable Fe-reducing bacterial abundance was four orders of magnitude greater in surface soil (0 – 0.1 m) than below 1 m. Although cultivable Fe oxidizing bacteria were typically also more abundant in surface soil, addition of labile C and nitrate stimulated Fe oxidizers in deep soil by two orders of magnitude under anaerobic conditions. This implies that infiltration of nitrate (and possibly C) from shallow soil water could potentially promote biotic Fe oxidation, a critical step in bedrock weathering, 7 m below. Together, these data suggest that C, Fe, and nutrient availability increase microbial Fe reduction and oxidation in surface (vs. deeper) soil microsites despite high bulk O_2, in contrast to the depth segregation of electron accepting processes often

observed in aquatic ecosystems. Furthermore, the greatest capacity for Fe redox cycling can occur in A horizons that do not display gleying or mottling.

Introduction

Iron (Fe) oxidation and reduction driven by microbial and/or abiotic processes are coupled to the biogeochemical cycling of carbon (C), phosphorus (P), nitrogen (N), and cations over ecological timescales, and contribute to mineral weathering and soil evolution over pedogenic timescales. Dissimilatory Fe reduction coupled to C oxidation is an important anaerobic microbial respiratory process, and dark Fe oxidation coupled to oxygen (O_2) or nitrate (NO_3^-) reduction can also support microbial growth (Weber et al. 2006; Melton et al. 2014). The ecosystem-scale importance of Fe redox cycling and its relationships to other elemental cycles have received greatest attention in aquatic sediments and wetland soils (Ponnamperuma 1972; Lovley 1995; Thamdrup 2000; Weber et al. 2006; Cheng et al. 2010). Yet, Fe redox cycling can also influence organic matter decomposition, nutrient dynamics, and mineral weathering in relatively well-drained surface soils of terrestrial ecosystems (Chacón et al. 2006; Thompson et al. 2006; Fimmen et al. 2008; Dubinsky et al. 2010; Hall and Silver 2013; Yang and Liptzin 2015). These dynamics are especially relevant in humid tropical soils, which are often rich in short-range-ordered Fe oxides and organic C. In these ecosystems, rates of soil Fe redox cycling and pools of reduced Fe (Fe(II)) often equal or exceed wetland sediments (Dubinsky et al. 2010; Thompson et al. 2011; Hall and Silver 2015). Yet, understanding the spatial distribution and controls on Fe reduction and oxidation in terrestrial soils remains an important knowledge gap hampering the incorporation of Fe redox cycling into quantitative and conceptual models of short

term (i.e., minutes – months) ecosystem dynamics, and long-term (i.e., centennial – millennial) weathering and pedogenic processes.

In aquatic sediments and groundwater, a dominant conceptual model proposes that respiratory terminal electron accepting processes exhibit an approximate segregation with depth according to their thermodynamic favorability. That is, given sufficient supply of C or other reductants, O_2 is rapidly reduced near the sediment surface, followed by the reduction of nitrate, manganese oxides, and Fe oxides in progressively deeper zones (Froelich et al. 1979; Chapelle et al. 1995; Roden and Wetzel 1996; Emerson and Hedges 2003). Thus, in undisturbed sediments we would typically expect respiratory Fe reduction to commence at depths where most O_2 has been depleted (Fig. 1a)—although sediment redox gradients can also be disrupted by bioturbation (Norkko et al. 2011). In terrestrial environments, spatial and temporal heterogeneity in O_2 availability is a common feature of soils undergoing fluctuations in moisture, C inputs, and biological activity. The importance of microsite-scale (mm – cm) redox gradients for stimulating denitrification in well-drained surface soils is widely acknowledged, and has been contrasted with the depth stratification of redox reactions in aquatic sediments (Seitzinger et al. 2006). Iron reduction also appears to be relatively commonplace in many well-drained surface soils (Silver et al. 1999; DeAngelis et al. 2010; Liptzin et al. 2011; Yang and Liptzin 2015), and even gross methane production can sometimes be measured in these systems (von Fischer and Hedin 2007). Despite these observations, patterns in the depth distribution of Fe redox cycling vis a vis availability of O_2 and other potential drivers (C, Fe, and N) have received much less attention in terrestrial soils.

Spatial interactions between controls on physical O_2 supply and biological O_2 demand may be crucial for understanding trends in Fe redox cycling with depth in terrestrial soils.

Macropore carbon dioxide (CO_2) concentrations typically increase with soil depth (Cerling 1991), corresponding to a stoichiometric decrease in O_2 that could stimulate Fe reduction with depth. Indeed, several studies have documented Fe reduction in subsoils (0.5 – 1.5 m) using morphological observations and geochemical analyses (Veneman et al. 1976; Fimmen et al. 2008; Schulz et al. 2016). The combination of periodically perched water and/or root C inputs to clay-rich subsurface horizons appeared to promote Fe reduction and oxidation in these studies (ibid.), generating prominent visual features of gleying and mottling indicative of Fe redox cycling. However, significant rates of Fe reduction can also occur in surface (A) soil horizons from a broad range of ecosystems (Chacón et al. 2006; Thompson et al. 2006; Dubinsky et al. 2010; Buettner et al. 2014; Yang and Liptzin 2015). At the surface, development of aggregates with tortuous diffusion paths allows anaerobic processes to occur in close spatial proximity to macropores with near-atmospheric O_2 concentrations (Sexstone et al. 1985). As a consequence, measurements of O_2 in soil macropores (defined here as "bulk O_2") do not necessarily reflect the prevalence of anaerobic microsites at small (mm – cm) spatial scales, despite their utility when comparing among sites over larger (m – km) spatial scales (Silver et al. 2013; Hall and Silver 2015; Liptzin and Silver 2015). Because both the availability of O_2 in soil macropores as well as total biological O_2 demand generally decrease with depth (Cerling 1991), the overall relationship between soil depth and Fe reduction remains unclear.

The availability of short-range-ordered Fe oxides, organic C, and co-limiting nutrients could also have a crucial impact on the depth distribution of Fe reduction. Humid tropical soils are often rich in Fe oxides, especially goethite and hematite, as a consequence of extensive weathering and desilication (Sanchez 1976; White et al. 1998). Yet, a relatively small fraction of total Fe may be readily accessible to Fe-reducing microbes. Iron reduction rates often scale with

111 the surface area and solubility of Fe oxide phases (Roden and Zachara 1996; Bonneville et al.
112 2009). The short-range-ordered Fe phases that dominate reducible Fe pools (Hyacinthe et al.
113 2006) may decline with depth (Thompson et al. 2011; Hall and Silver 2015), potentially limiting
114 Fe reduction. Organic C availability may also limit Fe reduction with depth. Humid tropical
115 forests are characterized by high C availability that fuels heterotrophic activity in surface soils
116 (Raich and Schlesinger 1992), and rates of Fe reduction appear tightly coupled with the
117 availability of dissolved organic C (Chacón et al. 2006; Fuss et al. 2010). Other nutrients such as
118 nitrogen (N) could also limit Fe reduction/oxidation, especially in deeper soil horizons with low
119 organic matter content. Even in comparatively N-rich tropical forests, N additions can enhance
120 particulate organic matter decomposition (Cleveland and Townsend 2006; Cusack et al. 2011),
121 and nutrient limitation may be exacerbated in comparatively resource-poor subsoils (Stone et al.
122 2014).

123 In deep soils, Fe(II) oxidation is also a crucial step in bedrock weathering, where
124 minerals such as hornblende and biotite provide a source of Fe(II) that can be oxidized via biotic
125 or abiotic mechanisms coupled to O_2 or NO_3^- (Buss et al. 2005; Fletcher et al. 2006; Liermann et
126 al. 2015). It has been hypothesized that O_2 availability limits mineral weathering at the interface
127 between bedrock and saprolite, and thus may play a key role in controlling landscape evolution
128 (Fletcher et al. 2006; Brantley and White 2009; Bazilevskaya et al. 2013; Behrens et al. 2015).
129 Oxygen concentrations often decrease with depth, reflecting a balance between diffusive supply
130 and the biological and geochemical processes that consume O_2. Fletcher et al. (2006) proposed
131 that depth-dependent decreases in O_2 served as a negative feedback on bedrock weathering,
132 given that increasing regolith thickness would presumably result in decreased O_2 supply at the

133 weathering front. Alternative oxidants such as NO_3^- could also potentially contribute to Fe(II)
134 oxidation (Böhlke et al. 2002; Liermann et al. 2015), especially under O_2-limited conditions.

135 Few studies have examined trends in O_2 and biogeochemical processes across deep soil
136 profiles. In Amazonian forests and pastures, soil CO_2 concentrations increased monotonically
137 with soil depth, implying a corresponding stoichiometric decline in O_2 from ~ 19 % above 1 m to
138 ~ 12 % at 8 m (Nepstad et al. 1994). Similarly, in a highly weathered Puerto Rican forest soil, O_2
139 declined from ~18% above 2 m to ~13% at 7 m (Liermann et al. 2015). It is unclear whether
140 changes in O_2 availability of this magnitude might impact biotic Fe(II) oxidation at depth, and
141 whether Fe-oxidizing microbial abundance might respond to availability of O_2, NO_3^-, or organic
142 matter.

143 We tested the hypothesis that microbial capacity for Fe reduction and oxidation across a
144 deep tropical forest soil profile correlates with depth variation in the availability of C and short-
145 range-ordered Fe as opposed to bulk soil O_2. In accordance with this hypothesis, we predicted
146 greater rates of Fe reduction and oxidation potential in surface as opposed to deeper soils, despite
147 a predicted decline in bulk soil O_2 with depth (Fig. 1b). This conceptual framework contrasts
148 with patterns often observed in flooded wetland soils and sediments (Fig. 1a). We predicted that
149 our terrestrial soils would deviate from this spatial segregation of aerobic and anaerobic
150 processes with depth, because of the importance of electron donor supply (i.e., organic C) in
151 generating anaerobic microsites where Fe reduction can occur within a porous soil matrix, as
152 well as an increased abundance of short-range-ordered Fe in surface soils. We also assessed the
153 degree to which addition of C, Fe, and NO_3^- affected Fe reduction and oxidation capacity across
154 the depth gradient. We predicted that NO_3^- addition would increase Fe oxidation capacity in deep

soils, where bedrock supplies ample Fe(II) but oxidant (O_2, NO_3^-) availability may limit rates of Fe(II) oxidation.

Methods

Site description

Samples were collected from the Guaba Ridge (18°17'02"N, 65°47'20"W) in the Río Icacos Watershed of the Luquillo Experimental Forest, Puerto Rico. This humid montane tropical forest ecosystem has mean annual temperature and precipitation of 22 ºC and 4200 mm, respectively (White et al. 1998). Despite high precipitation, surface soils (0 - 10 cm) remain well drained due to high porosity (~75 %; White et al. 1998) and bioturbation. Parent material is quartz diorite from the Rio Blanco stock, dominated by plagioclase feldspar and quartz (White et al. 1998). Soils in the watershed include Oxisols, Ultisols, and Inceptisols, and vary according to topographic position (Soil Survey Staff 2002; Johnson et al. 2015). The Guaba Ridge separates two first-order streams that discharge to the Río Icacos at approximately 650 m elevation. The soil sampled here was recently characterized as a Plinthic Haplohumult (Yi-Balan et al. 2014), similar to the Humic Hapludox described by the Soil Survey Staff (2002). The B horizons transition to saprolite at a depth of approximately 1 m (White et al. 1998; Yi-Balan et al. 2014). Gleying indicative of Fe reduction was especially prominent between 0.2 and 0.4 m. Fine root biomass was greatest from 0 – 10 cm and declined precipitously with depth, and was absent below 80 cm (Johnson et al. 2015; Hall and Silver 2015). Organic C declined with depth from 2 – 3 % C by mass from 0 – 0.1 m (S. J. Hall, unpublished data), to 1.6, 1.5, 1.2, and 1.1 % C at depths of 0.15, 0.3, 0.45, and 0.6 m, respectively. Below 0.6 m, C was typically < 0.2 % (Buss et

al. 2005). Clay-sized particles were most abundant (42 %) at 0.3 m, and measured between 16 and 30 % in other samples to 5 m depth (Buss et al. 2005). Total Fe oxide content (as Fe_2O_3) increased from ~ 4 % at the surface to > 7 % at depth (White et al. 1998). Site vegetation was evergreen tropical montane forest locally described as the "palo colorado" forest, after the dominant species *Cyrilla racemiflora* L. (Weaver and Murphy 1990).

Soil sampling

Soils were sampled on two separate occasions using a 7.6 cm diameter stainless steel bucket auger and extensions. Samples at a given depth interval represent composites from three separate augured holes collected within a radius of 15 m. The 2010 samples were collected from depth increments of 0 – 0.15, 1.5 – 1.8, and 6.9 – 7.2 m. The 2012 samples were collected from 0 – 0.1, 0.1 – 0.2, 0.2 – 0.5, 0.5 – 1, 1 – 2, 2 – 3, 3 – 4, and 4 – 5 m. Samples were stored at field moisture in sealed polyethylene bags at ambient temperature (22 – 25 °C).

Oxygen measurements

We installed O_2 sensors (Apogee SO-110, Logan UT) at depths of 0.1, 0.25, 0.5, 1, 2, 3, 4, and 5 m in June 2010 and monitored them until February 2012. Sensors were calibrated at 100 % relative humidity prior to installation and upon retrieval, and corrected for linear drift over time. Each sensor was installed in a separate hole augured to the depth of installation. Holes were separated laterally by > 1 m. Sensors were deployed inside 10 cm lengths of 5.1 cm diameter polyvinylchloride pipe sealed with a cap on the top and bottom and perforated on the sides with 0.5 cm diameter holes to allow gas exchange with the adjacent soil atmosphere. After lowering a sensor to the bottom of the augured hole, soil was refilled and tamped above the sensor to approximate field bulk density using a stainless steel rod. The initial week of data was discarded,

after which point O_2 concentrations (atmospheric mixing ratios) established pseudo steady-state values at deeper depths. Data were recorded at hourly intervals on a datalogger (CR1000, Campbell Scientific, Logan UT) during most of the 21-month period. Continuous measurements were not possible due to remote nature of the field site and associated battery failure.

Chemical analyses and laboratory experiments

We measured Fe and trace gas production in the laboratory at U. C. Berkeley shortly after soils were sampled, and during the course of two laboratory experiments. Iron(II) and (III) were measured in 0.5M HCl extractions using a 1:10 mass ratio of soil to solution, denoted as $Fe(II)_{HCl}$ and $Fe(III)_{HCl}$. Soils were extracted for two hours on a rotary shaker, centrifuged at 3200 rcf, and the supernatant solution filtered to 0.2 µm. Solutions were analyzed using a modified ferrozine method (Viollier et al. 2000). Here, we used $Fe(III)_{HCl}$ as an index of short-range-ordered Fe oxides. Our previous work at nearby sites showed a strong correlation between $Fe(III)_{HCl}$ and Fe extracted via reductive dissolution with citrate-ascorbate solution, although $Fe(III)_{HCl}$ was always of smaller magnitude (Hall and Silver 2015). Citrate-ascorbate extractable Fe is thought to be closely correlated with microbially-reducible Fe (Hyacinthe et al. 2006). We measured production of carbon dioxide (CO_2) using gas chromatography (Shimadzu 14A, Columbia MD) as described previously (Hall et al. 2013).

We tested relationships between bulk soil O_2, trace gas production, and Fe_{HCl} across soils from 0 – 5 m depth (0 – 0.1, 0.1 – 0.2, 0.2 – 0.5, 0.5 – 1, 1 – 2, 2 – 3, 3 – 4, and 4 – 5 m). Samples (~15 g dry mass equivalent) were incubated in glass jars for 24 hours in darkness under an ambient atmosphere (20.9 % O_2) within 7 days of sample collection, with three replicates per depth. We report $Fe(II)_{HCl}$ and $Fe(III)_{HCl}$ extracted immediately prior to the trace gas

221 measurements. Next, we incubated a subset of these soils (0.1 – 0.2, 0.5 – 1, 2 – 3, 3 – 4, 4 – 5 m
222 depths) under hypoxic (N_2 headspace) and aerobic conditions (~20.9 % O_2) over 10-days to
223 assess potential rates of Fe reduction (n = 3 per depth and headspace).

224 Together, these measurements identified surface soil horizons as a dominant zone of
225 actual and potential Fe reduction. We then tested the importance of labile C and short-range-
226 ordered Fe availability as controls on Fe reduction in 0 – 0.1 m soil using a full factorial
227 experiment (n = 3 per treatment) conducted under hypoxic conditions (N_2 headspace) to simulate
228 the presence of reducing microsites under field conditions. Short-range-ordered Fe as hydrous
229 ferric oxide (HFO) was prepared as described previously (Yang et al. 2012) and gently
230 homogenized with soil subsamples (~ 15 g dry mass equivalent) at concentrations of 0, 0.1, 0.5,
231 and 1 mg Fe g $soil^{-1}$. Labile C was added as glucose dissolved in deionized water at
232 concentrations of 0, 50, 100, and 200 µg C g $soil^{-1}$. Glucose was used given that it can be
233 fermented to multiple compounds that support Fe reduction (Lovley 1995).

234 Finally, we used separate samples spanning the soil surface to bedrock to further test
235 environmental controls on Fe reduction, as well as the abundance of Fe reducing and oxidizing
236 bacteria using most probable number (MPN) analyses as described by Dubinsky et al. (2010).
237 Soils from 0 – 0.15, 1.5 – 1.8, and 6.9 – 7.2 m depths were combined in a 1:2 ratio with
238 deionized water and incubated under anaerobic conditions for 8 days. This experiment was
239 designed to assess controls on Fe cycling under anaerobic conditions, to test impacts of NO_3^-
240 availability on Fe oxidation, and to compare with an aerobic pre-treatment control. Soil solutions
241 were amended with either sodium nitrate (NO_3^-; 1 mM final concentration), Fe as ferrous
242 chloride (2 mM), Fe + NO_3^-, sodium acetate (0.5 mM), and acetate + NO_3^-, or deionized water,
243 and incubated in an anaerobic chamber (90% N_2, 8% CO_2, and 2% H_2 headspace). Acetate was

used in this experiment given the precedence of studies that successfully cultivated Fe oxidizers and reducers (Lovley 1995; Straub et al. 1996). To enumerate anaerobic Fe reducing and oxidizing bacteria, soils were extracted in buffer containing 0.1% sodium pyrophosphate and 0.03% Tween 80 in basal microbiological medium (BMM). BMM consisted of (per L) 5.0 g 2-(N-morpholino)ethanesulfonic acid (MES) buffer and 10 ml mineral solution, with 0.80 g NaCl, 1.0 g NH_4Cl, 0.1 g KCl, 0.1 g KH_2PO_4, 0.2 g $MgCl_2 \cdot 6H_2O$, and 0.04 g $CaCl_2 \cdot 2H_2O$ (per L). After autoclaving, the media pH was adjusted to 5.5 and amended with 1 ml SL12 trace elements solution, 2.5 ml trace metal solution (Widdel and Bak 1992), and 1 ml vitamin solution (Pfennig and Trüper 1992) per L. Media was dispensed into 96-well microplates, and soil subsamples added in ten-fold dilutions from 10^{-2} to 10^{-13} with four biological replicates and three technical replicates per depth per amendment. Plates were incubated in the dark for 30 days with negative controls including soil extract buffer only (no soil). Positive growth of Fe(III) reducers was visualized by adding ferrozine solution, which turns purple in the presence of Fe(II). Formation of reddish-brown precipitates was used to verify positive results for Fe(II) oxidizers. Cell counts per gram of soil were calculated using the Most Probable Number Calculator version 4.04 (Klee 1996).

For all experiments, statistical differences among treatments and/or depths were assessed using ANOVA and post-hoc Tukey comparisons using R v. 3.2.0. To account for temporal autocorrelation in the O_2 data, we used a generalized linear model with an autoregressive error term implemented using the glm function.

Results

Median bulk soil O_2 concentrations (mixing ratios) exceeded 16 % at all depths measured between 0.10 and 5 m (Fig. 2a). All depths significantly differed ($p < 0.05$) from each other with the exception of the 1 and 4 m depths. However, differences in O_2 were often small: below 0.5 m, median O_2 concentrations differed by < 0.3 % and did not consistently decrease with depth (Fig. 2a). Oxygen was most dynamic at 0.25 and 0.5 m depths, where O_2 varied by as much as 10 % over time (Fig. 2a). In contrast, depths below 0.5 m showed much less variability (< 1.5 % O_2) relative to median values.

Concentrations of $Fe(II)_{HCl}$ and $Fe(III)_{HCl}$ measured on soils sampled in May 2012 showed different patterns from bulk soil O_2 (Fig. 2). $Iron(II)_{HCl}$ was greatest in 0 – 0.1 m soil and declined precipitously with depth, and was negligible below 1 m (Fig. 2b). Concentrations of $Fe(III)_{HCl}$ showed very similar depth trends as $Fe(II)_{HCl}$ (Fig. 2c). Patterns of short-term CO_2 production closely mirrored both $Fe(II)_{HCl}$ and $Fe(III)_{HCl}$ (Fig. 2d), and rates declined > 10-fold between the 0 – 0.1 and 0.5 – 1 m depths. Ten-day anaerobic incubations of a subset of these soils confirmed that potential Fe reduction was greatest in the most shallow soil tested (0.1 – 0.2 m), declined by an order of magnitude between 0.5 and 3 m, and was undetectable (not different from zero, $p > 0.05$) from 3 to 5 m (Fig. 3). Samples incubated under an *aerobic* atmosphere displayed no significant net change in Fe(II) concentrations over this time period (data not shown).

Factorial incubation experiments with 0 – 0.1 m soil indicated that Fe reduction generally increased with increased rates of labile C addition (glucose) under anaerobic conditions. Production of $Fe(II)_{HCl}$ was significantly greater ($p < 0.05$) in samples that received the highest glucose concentrations (100 and 200 µg C g $soil^{-1}$) and no or minimal Fe(III) addition (0 and 0.1 mg Fe g $soil^{-1}$). Iron(III) addition had no significant effect on $Fe(II)_{HCl}$ production in the

288 treatments with no or minimal glucose addition (0 and 50 μg C g soil^{-1}). However, the treatments
289 with the highest Fe concentrations decreased $Fe(II)_{HCl}$ production relative to the controls. This
290 effect depended on the amount of added glucose (Fig. 4; treatment interaction $p < 0.0001$).
291 Addition of 1 mg Fe g soil^{-1} decreased $Fe(II)_{HCl}$ production in the presence of 100 μg glucose C
292 g soil^{-1}, whereas 0.5 mg Fe g soil^{-1} decreased $Fe(II)_{HCl}$ production with 200 μg glucose C g soil^{-1}.

293 In our final experiment, we incubated soil slurries from surface, intermediate, and deep
294 samples (0 – 0.15, 1.5 – 1.8, and 6.9 – 7.2 m) to test the factors controlling the abundance of Fe
295 reducing and oxidizing organisms under anaerobic conditions, simulating anaerobic microsites in
296 the field. Iron reduction rates were two orders of magnitude greater in surface than deeper
297 samples ($p < 0.001$), although lower but significant rates of Fe reduction were also detectable in
298 some of the intermediate and deep samples under these experimental conditions (Fig. 5a, note the
299 log scale). Trends in Fe reduction rates with depth were corroborated by MPN analyses of
300 cultivable Fe reducers, which were four orders of magnitude greater in surface than deeper
301 samples (Fig. 5b). Experimental amendments (acetate, Fe, and NO_3^-) did not significantly affect
302 Fe reduction rates in surface (0 – 0.15 m) samples. However, Fe + NO_3^- addition increased the
303 abundance of cultivable Fe reducers three-fold relative to the controls in these samples ($p < 0.05$;
304 Fig. 5b). Nitrate addition alone doubled mean cultivable Fe reducer abundance relative to the
305 control in surface soil, but this difference was not statistically significant. In the intermediate
306 depth samples (1.5 – 1.8 m), addition of Fe, Fe + NO_3^-, acetate, and acetate + NO_3^- all
307 significantly stimulated Fe reduction rates relative to the control, but had no significant impact
308 on Fe reducer MPN (Fig. 5a,b), where abundances were low across all treatments. Iron + NO_3^-
309 addition stimulated Fe reduction rates in the intermediate depth samples to the greatest extent (p

310 < 0.05). In the deep soil samples (6.9 – 7.2 m), Fe and Fe + NO_3^- stimulated Fe reduction relative
311 to the controls, whereas the other treatments had no significant effects.

312 Iron(II) oxidizers were most abundant in surface soils at the beginning of the experiment,
313 and Fe oxidizer MPN was not significantly affected by experimental amendments in either the
314 surface or intermediate samples (Fig. 5c). In the deep samples, addition of acetate + NO_3^- (but
315 not acetate or NO_3^- alone) significantly stimulated Fe oxidation MPN by two orders of
316 magnitude relative to the other treatments. Notably, Fe oxidizer MPN values were not inhibited
317 by anaerobiosis per se at any depth, as they did not decrease relative to initial values under any
318 treatment despite incubation under anaerobic conditions.

319

320 **Discussion**

321 Our data support the hypothesis that labile C and Fe availability (Fig. 1b), as opposed to
322 variation in bulk O_2 with depth (Figs. 1a, 2), controlled Fe reduction across this deep humid
323 tropical forest soil profile. Actual and potential Fe reduction and cultivable Fe reducer abundance
324 were greatest in surface soils where bulk O_2 concentrations were also highest (Figs. 2,3). Iron
325 reduction declined by two orders of magnitude below 1 m despite decreased bulk soil O_2, and
326 cultivable Fe reducer abundance declined by four orders of magnitude. Soil respiration (Fig. 2)
327 and bulk soil C (Buss et al. 2005) showed a depth pattern similar to Fe reduction, and addition of
328 labile C (but not Fe) significantly enhanced Fe reduction in surface soil (Fig. 4). Apparent
329 decreases in $Fe(II)_{HCl}$ production at the highest concentrations of added Fe and glucose (Fig. 4)
330 may represent Fe(II)-catalyzed transformation of short-range-ordered Fe into more crystalline
331 phases that occluded the newly-produced Fe(II) (Jeon et al. 2003). Although these data represent

a single site, they support our proposed conceptual framework as well as the need to more broadly reconsider the controls and impacts of Fe redox cycling with depth, as discussed below.

Contrasting depth distribution of Fe redox cycling in wetlands and uplands

A dominant conceptual model in aquatic sediments posits that terminal electron accepting processes are segregated with depth according to their thermodynamic favorability (Emerson and Hedges 2003; Fig. 1a). However, our data suggest that this model does not necessarily explain depth variation in Fe reduction and oxidation potential at our site, and perhaps also in other well-drained terrestrial soils where high Fe reduction capacity has been documented (Yang and Liptzin 2015). Bulk O_2, Fe(II) concentrations, and potential Fe reduction were all greatest at the surface, concomitant with greatest labile C availability. These observations, combined with our experimental data, suggest that patterns in electron donor (i.e., organic C) availability provide a proximate control on the depth distribution of Fe reduction in this soil.

Although bulk O_2 concentrations declined with depth below 0.25 m, the abundance of anaerobic microsites also declined along with C availability, as reflected by lower concentrations of Fe(II), lower potential Fe reduction rates, and lower abundance of Fe-reducing and oxidizing microbes. Subtly increased O_2 concentrations at 0.25 m relative to 0.1 m likely reflected lateral spatial heterogeneity in soil O_2 (Liptzin et al. 2011; Hall et al. 2013) as opposed to a consistent trend with depth. Contrasting patterns between the depth distribution of terminal electron accepting processes in aquatic sediments vs. this terrestrial forest point to the importance of microsite-scale anaerobic processes within the largely aerobic soil matrix (Sexstone et al. 1985; Hall and Silver 2015; Keiluweit et al. 2016). Localized inputs of labile C to fuel O_2 consumption may be a critical regulator of the abundance of anaerobic microsites (Chacón et al. 2006),

evidenced by recent reports of Fe reduction associated with the rhizosphere (Fimmen et al. 2008; Schulz et al. 2016). In many ecosystems, including this humid tropical forest, root biomass C inputs are greatest near the soil surface (Jobbagy and Jackson 2000; Hall and Silver 2015). Thus, we predict that Fe redox cycling and the numerous processes linked to these dynamics—e.g., sorption and desorption of P and organic matter (Peretyazhko and Sposito 2005; Chacón et al. 2006; Thompson et al. 2006; Buettner et al. 2014; Hall et al. 2016), microbial respiration (Dubinsky et al. 2010), and production of reactive oxygen species (Hall and Silver 2013)—may also be most significant near the surface of many other terrestrial soils, despite the fact that moisture and visual indicators of Fe redox cycling often increase with depth.

Cryptic Fe redox cycling in surface soils

Our finding of greater Fe reduction capacity in surface vs. subsurface soils shows that trends in soil coloration and moisture are not necessarily reliable indicators of potential *rates* of Fe redox cycling. The greatest Fe(II) concentrations, potential rates of Fe reduction, and abundance of cultivable microbial Fe reducers and oxidizers occurred in surface A horizon (0 – 0.1 m) soil, where porosity was high (~ 75 %) and moisture rarely approached saturation (White et al. 1998). In this soil, gleying was visible throughout the B horizons, but not in the A horizon (Yi-Balan et al. 2014). Surface horizons were rarely saturated, and water content was typically greatest near the soil-saprolite interface (White et al. 1998). Investigations of Fe reduction in terrestrial soils have often focused on Fe redox dynamics in relatively deeper (> 0.5 m) B horizons associated with periodic moisture saturation and rhizosphere gleying (Veneman et al. 1976; Fimmen et al. 2008; Schulz et al. 2016). Mottling and gleying provide important visual evidence of Fe reduction, translocation, and oxidation (Veneman et al. 1976; Fimmen et al. 2008; Schulz et al. 2016). Although these features are *sufficient* to indicate the occurrence of Fe redox

377 cycling, they are not obligate indicators, as demonstrated by our data. Several studies have
378 similarly demonstrated high rates of Fe reduction at the soil surface (Chacón et al. 2006;
379 Dubinsky et al. 2010; Yang and Liptzin 2015) but did not assess trends with depth. Visual
380 evidence of Fe redox cycling in 0 – 0.1 m soil may have been obscured by high organic matter
381 content at the surface, which imparts a dark color. Surface soil horizons typically contain the
382 highest stocks of root biomass and organic C across a broad range of terrestrial ecosystems
383 (Jobbagy and Jackson 2000). As a consequence of abundant C inputs that generate anaerobic
384 microsites yet obscure the visual effects of Fe reduction, we suggest that cryptic Fe reduction in
385 terrestrial surface soils may be a more commonplace phenomenon than is implied by visible
386 gleying and mottling.

387 In surface soils of humid tropical forests and other terrestrial ecosystems, hotspots of Fe
388 reduction in surface soil microsites are likely generated due to the confluence of several critical
389 factors. High clay content decreases gas-phase diffusivity and O_2 supply, high temperature
390 decreases O_2 solubility while increasing biological O_2 consumption, a high density of live and
391 dead roots provides abundant C inputs, and large pools of Fe are maintained in short-range-
392 ordered minerals (Silver et al. 1999; Buss et al. 2005; Thompson et al. 2011; Johnson et al. 2015;
393 Hall and Silver 2015). The maintenance of short-range-ordered Fe appears critical in that these
394 phases exhibit greater rates of reduction than crystalline Fe (Roden and Wetzel 2002).
395 Interactions between Fe and organic matter likely retard the formation of crystalline minerals
396 (Schwertmann et al. 1988), despite the fact that redox cycling can potentially lead to formation
397 of Fe with greater crystalline structure (Thompson et al. 2006). At depth, lower organic matter
398 concentrations may facilitate the formation of more crystalline Fe minerals during redox cycling
399 (Jeon et al. 2003; Thompson et al. 2006), consistent with previous Fe isotope measurements at

this site (Buss et al. 2010). This coincides with our finding that Fe addition stimulated Fe reduction at depth (Fig. 5), despite the presence of a large total Fe oxide pool (White et al. 1998).

Implications of O_2 depth distribution for bedrock weathering

Bulk soil O_2 concentrations did not consistently decrease with depth below 1 m, the approximate depth of the soil/saprolite transition, but rather fluctuated around similar median values (~ 16 %; Fig. 2). Previous work hypothesized that regolith depth controls weathering rates by constraining O_2 supply, given that O_2 availability may limit oxidation of Fe in primary bedrock minerals (Fletcher et al. 2006; Brantley and White 2009; Behrens et al. 2015). A key assumption of this hypothesis is that O_2 concentrations decrease monotonically with regolith depth, facilitating a negative feedback between regolith development and weathering rates. Our data show that bulk soil O_2 does not necessarily decrease consistently or significantly within the saprolite profile. Rather, the asymptotic trend in bulk soil O_2 observed here at depths below 1 m is consistent with analytical models of soil CO_2 production and diffusion (Cerling 1991; Fig. 1b) validated by measurements in shallower soil profiles (< 1.5 m depth) from other ecosystems (e.g. Solomon and Cerling 1987; Bowling et al. 2015). Bulk O_2 concentrations observed here at 5 m depth (~16 %), as well as other tropical forests (~12 – 17 %; Nepstad et al., 1994; Liermann et al., 2015), were relatively high. If these data and models are broadly representative, regolith depth per se may not necessarily influence gas-phase O_2 supply to the bedrock/saprolite interface. Rather, the presence and depth of perched water tables at the bedrock/saprolite interface (White et al. 1998) may be more important in controlling diffusive O_2 supply for primary mineral weathering.

Potential importance of anaerobic Fe oxidation at depth

Although bulk soil O_2 concentrations were relatively high in deep soils, anaerobic microsites are likely to occur (Silver et al. 1999), particularly in the presence of perched water tables at the bedrock interface (White et al. 1998; Schulze and White 1999). Iron(II) oxidation by NO_3^- can be a significant process in shallow groundwater (Böhlke et al. 2002). As a consequence, availability of both O_2 and NO_3^- could potentially influence rates of Fe(II) oxidation at the bedrock/saprolite weathering front. In our study, Fe(II) oxidation at intermediate depths was likely limited by Fe(II) supply from primary minerals (Buss et al. 2005) and the abundance of cultivable Fe(II) oxidizers was unaffected by our experimental treatments. In deep soils, cultivable Fe(II) oxidizer abundance was initially similar to intermediate depths, but responded strongly to additions of NO_3^- and acetate under anaerobic conditions—increasing by two orders of magnitude relative to initial aerobic conditions. This finding suggests significant capacity for anaerobic, microbially-mediated Fe(II) oxidation in deep soils.

We note that our results are likely conservative in that the MPN enumeration method used here yielded *cultivable* anaerobic Fe reducers and oxidizers, and likely underestimates their total populations (Dubinsky et al. 2010). Previous work in nearby soils found that cultivable Fe reducers represented 0.7 – 5.7 % of total bacterial abundance, but that the relative abundances of the canonical Fe reducers *Shewanella* and *Geobacter* assessed were low when assessed using quantitative PCR (Dubinsky et al. 2010; DeAngelis et al. 2010). The composition of Fe reducing and oxidizing microbial communities in humid tropical soils remains poorly understood.

The finding that acetate stimulates anaerobic Fe(II) oxidizers suggests that heterotrophic or mixotrophic Fe oxidizers contribute to Fe(II) oxidation and related bedrock weathering at depth. Previous studies similarly found that C addition enhanced rates of Fe(II) oxidation (Straub et al. 1996; Kappler et al. 2005). The stimulatory effect of acetate on Fe(II) oxidizer abundance

445 may reflect the importance of mixotrophy in preventing the deleterious effects of cell
446 encrustation by the newly-formed Fe(III) oxides (Kappler et al. 2005). However, the finding that
447 acetate stimulated Fe(II) oxidizer abundance presents an interesting conundrum: previous
448 measurements suggested that deep dissolved organic C concentrations may be extremely low at
449 this site (Schulz and White 1999), supporting the hypothesis that microbial communities are
450 dominated by autotrophs reliant on bedrock Fe(II) supply and are decoupled from surface C
451 inputs (Liermann et al. 2015). Yet, the strong response of cultivable Fe oxidizers to C addition in
452 deep soils also suggests that heterotrophic microbial communities are poised to respond to C
453 inputs, either from co-occurring autotrophs or possibly from surface soils.

454 The observation of high NO_3^- concentrations (~ 20 µM) in deep soils from this site and
455 another nearby site (Schulz and White 1999; Liermann et al. 2015) is indicative of hydrologic
456 NO_3^- supply from surface soils 7 m above, as the parent material does not contain significant N
457 (White et al. 1998). Surface soil biological processes do not appear strongly N limited in this
458 ecosystem (Cusack et al. 2011), thus infiltration of surface soil NO_3^- to deep soils appears
459 plausible. The potential for surface soil dissolved organic matter to reach the weathering front at
460 7 m depth without being sorbed or mineralized in transit may be more tenuous. Couplings
461 between surface-derived nutrients and bedrock weathering remain an important but poorly
462 explored topic in the context of landscape evolution, and biogeochemical connections between
463 surface and deep subsurface soils merit further exploration.

464

465 **Conclusions**

Trends in potential Fe reduction and oxidation varied systematically with depth in this terrestrial humid tropical forest soil but showed distinctly different trends compared to the standard conceptual model for saturated sediments. Although mean bulk O_2 declined overall with depth, it was most variable and sporadically reached the lowest values at shallow depths (0.25 and 0.5 m). Biotic Fe reduction and oxidation capacity were greatest at the surface and declined precipitously with depth. At intermediate and deep depths, Fe reduction and oxidation appeared strongly limited by C, NO_3^-, and/or labile Fe, despite high total Fe. However, biotic Fe oxidation potential increased at the saprolite/bedrock interface in response to acetate and NO_3^- addition, likely as a consequence of increased Fe(II) supply from primary Fe(II)-rich minerals, which had been depleted from shallower saprolite (intermediate depths). Shallow surface soils may play an underappreciated role as hotspots of coupled Fe reduction and oxidation, even when visible gleying is not apparent. Furthermore, our data suggest that the total depth of soil profiles may have less influence on bulk O_2 supply to bedrock than previously proposed, given the observed asymptotic trend in O_2 with depth. In addition to O_2 availability, we showed that the supply of NO_3^- from surface soils could play an important role in bedrock weathering by stimulating Fe(II) oxidizing microbial communities. Although labile C amendments stimulated the growth of Fe(II) oxidizers, it remains uncertain whether surface soil inputs provide a significant C source at 7 m depth.

Acknowledgements

Data associated with this manuscript will be available on the Luquillo CZO data repository (http://criticalzone.org/luquillo/data/) after publication. We thank Heather Dang and Andrew

488 McDowell for crucial help in the lab, and Manual Rosario for data collection. We thank Aaron
489 Thompson for providing valuable insights on this work. This work was supported by NSF grant
490 DEB-1457805 to WLS and SJH, and the NSF Luquillo Critical Zone Observatory (EAR-
491 0722476) and LTER (DEB-0620910).

492 **References**

493 Bazilevskaya E, Lebedeva M, Pavich M, et al (2013) Where fast weathering creates thin regolith
494 and slow weathering creates thick regolith. Earth Surf Process Landf 38:847–858. doi:
495 10.1002/esp.3369

496 Behrens R, Bouchez J, Schuessler JA, et al (2015) Mineralogical transformations set slow
497 weathering rates in low-porosity metamorphic bedrock on mountain slopes in a tropical
498 climate. Chem Geol 411:283–298. doi: 10.1016/j.chemgeo.2015.07.008

499 Böhlke JK, Wanty R, Tuttle M, et al (2002) Denitrification in the recharge area and discharge
500 area of a transient agricultural nitrate plume in a glacial outwash sand aquifer, Minnesota.
501 Water Resour Res 38:10–1. doi: 10.1029/2001WR000663

502 Bonneville S, Behrends T, Van Cappellen P (2009) Solubility and dissimilatory reduction
503 kinetics of iron(III) oxyhydroxides: A linear free energy relationship. Geochim
504 Cosmochim Acta 73:5273–5282. doi: 10.1016/j.gca.2009.06.006

505 Bowling DR, Egan JE, Hall SJ, Risk DA (2015) Environmental forcing does not induce diel or
506 synoptic variation in the carbon isotope content of forest soil respiration. Biogeosciences
507 12:5143–5160. doi: 10.5194/bg-12-5143-2015

508 Brantley SL, White AF (2009) Approaches to modeling weathered regolith. Rev Mineral
509 Geochem 70:435–484. doi: 10.2138/rmg.2009.70.10

510 Buettner SW, Kramer MG, Chadwick OA, Thompson A (2014) Mobilization of colloidal carbon
511 during iron reduction in basaltic soils. Geoderma 221–222:139–145. doi:
512 10.1016/j.geoderma.2014.01.012

513 Buss HL, Bruns MA, Schultz MJ, et al (2005) The coupling of biological iron cycling and
514 mineral weathering during saprolite formation, Luquillo Mountains, Puerto Rico.
515 Geobiology 3:247–260. doi: 10.1111/j.1472-4669.2006.00058.x

516 Buss HL, Mathur R, White AF, Brantley SL (2010) Phosphorus and iron cycling in deep
517 saprolite, Luquillo Mountains, Puerto Rico. Chem Geol 269:52–61. doi:
518 10.1016/j.chemgeo.2009.08.001

519 Cerling TE (1991) Carbon dioxide in the atmosphere; evidence from Cenozoic and Mesozoic
520 Paleosols. Am J Sci 291:377–400. doi: 10.2475/ajs.291.4.377

521 Chacon N, Silver WL, Dubinsky EA, Cusack DF (2006) Iron reduction and soil phosphorus
522 solubilization in humid tropical forest soils: The roles of labile carbon pools and an
523 electron shuttle compound. Biogeochemistry 78:67–84. doi: 10.1007/s10533-005-2343-3

524 Chapelle FH, McMahon PB, Dubrovsky NM, et al (1995) Deducing the distribution of terminal
525 electron-accepting processes in hydrologically diverse groundwater systems. Water
526 Resour Res 31:359–371.

527 Cheng L, Zhu J, Chen G, et al (2010) Atmospheric CO2 enrichment facilitates cation release
528 from soil. Ecol Lett 13:284–291. doi: 10.1111/j.1461-0248.2009.01421.x

529 Cleveland CC, Townsend AR (2006) Nutrient additions to a tropical rain forest drive substantial
530 soil carbon dioxide losses to the atmosphere. Proc Natl Acad Sci 103:10316–10321. doi:
531 10.1073/pnas.0600989103

532 Cusack DF, Silver WL, Torn MS, McDowell WH (2011) Effects of nitrogen additions on above-
533 and belowground carbon dynamics in two tropical forests. Biogeochemistry 104:203–225.
534 doi: 10.1007/s10533-010-9496-4

535 DeAngelis KM, Silver WL, Thompson AW, Firestone MK (2010) Microbial communities
536 acclimate to recurring changes in soil redox potential status. Environ Microbiol 12:3137–
537 3149. doi: 10.1111/j.1462-2920.2010.02286.x

538 Dubinsky EA, Silver WL, Firestone MK (2010) Tropical forest soil microbial communities
539 couple iron and carbon biogeochemistry. Ecology 91:2604–2612. doi: 10.1890/09-1365.1

540 Emerson S, Hedges J (2003) Sediment diagenesis and benthic flux. Treatise Geochem 6:293–319.
541 doi: 10.1016/B0-08-043751-6/06112-0

542 Fimmen RL, Richter D deB, Vasudevan D, et al (2008) Rhizogenic Fe–C redox cycling: a
543 hypothetical biogeochemical mechanism that drives crustal weathering in upland soils.
544 Biogeochemistry 87:127–141.

545 Fletcher RC, Buss HL, Brantley SL (2006) A spheroidal weathering model coupling porewater
546 chemistry to soil thicknesses during steady-state denudation. Earth Planet Sci Lett
547 244:444–457. doi: 10.1016/j.epsl.2006.01.055

548 Froelich PN, Klinkhammer GP, Bender ML, et al (1979) Early oxidation of organic matter in
549 pelagic sediments of the eastern equatorial Atlantic: suboxic diagenesis. Geochim
550 Cosmochim Acta 43:1075–1090. doi: 10.1016/0016-7037(79)90095-4

551 Fuss CB, Driscoll CT, Johnson CE, et al (2010) Dynamics of oxidized and reduced iron in a
552 northern hardwood forest. Biogeochemistry 104:103–119. doi: 10.1007/s10533-010-
553 9490-x

554 Hall SJ, McDowell WH, Silver WL (2013) When wet gets wetter: Decoupling of moisture, redox
555 biogeochemistry, and greenhouse gas fluxes in a humid tropical forest soil. Ecosystems
556 16:576–589. doi: 10.1007/s10021-012-9631-2

557 Hall SJ, Silver WL (2013) Iron oxidation stimulates organic matter decomposition in humid
558 tropical forest soils. Glob Change Biol 19:2804–2813. doi: 10.1111/gcb.12229

559 Hall SJ, Silver WL (2015) Reducing conditions, reactive metals, and their interactions can
560 explain spatial patterns of surface soil carbon in a humid tropical forest. Biogeochemistry
561 125:149–165. doi: 10.1007/s10533-015-0120-5

562 Hall SJ, Silver WL, Timokhin VI, Hammel KE (2016) Iron addition to soil specifically stabilized
563 lignin. Soil Biol Biochem 98:95–98. doi: 10.1016/j.soilbio.2016.04.010

564 Hyacinthe C, Bonneville S, Van Cappellen P (2006) Reactive iron(III) in sediments: Chemical
565 versus microbial extractions. Geochim Cosmochim Acta 70:4166–4180. doi:
566 10.1016/j.gca.2006.05.018

567 Jeon B-H, Dempsey BA, Burgos WD (2003) Kinetics and mechanisms for reactions of Fe(II)
568 with iron(III) oxides. Environ Sci Technol 37:3309–3315. doi: 10.1021/es025900p

569 Jobbagy EG, Jackson RB (2000) The vertical distribution of soil organic carbon and its relation
570 to climate and vegetation. Ecol Appl 10:423–436. doi: 10.1890/1051-
571 0761(2000)010[0423:TVDOSO]2.0.CO;2

572 Johnson AH, Xing HX, Scatena FN (2015) Controls on soil carbon stocks in El Yunque National
573 Forest, Puerto Rico. Soil Sci Soc Am J 79:294. doi: 10.2136/sssaj2014.05.0199

574 Kappler A, Schink B, Newman DK (2005) Fe(III) mineral formation and cell encrustation by the
575 nitrate-dependent Fe(II)-oxidizer strain BoFeN1. Geobiology 3:235–245. doi:
576 10.1111/j.1472-4669.2006.00056.x

577 Keiluweit M, Nico PS, Kleber M, Fendorf S (2016) Are oxygen limitations under recognized
578 regulators of organic carbon turnover in upland soils? Biogeochemistry 1–15. doi:
579 10.1007/s10533-015-0180-6

580 Klee AJ (1996) Most Probable Number Calculator. US Environmental Protection Agency, Risk
581 Reduction Engineering Laboratory, Cincinnati, OH, USA

582 Liermann LJ, Albert I, Buss HL, et al (2015) Relating microbial community structure and
583 geochemistry in deep regolith developed on volcaniclastic rock in the Luquillo
584 Mountains, Puerto Rico. Geomicrobiol J 32:494–510. doi:
585 10.1080/01490451.2014.964885

586 Liptzin D, Silver WL (2015) Spatial patterns in oxygen and redox sensitive biogeochemistry in
587 tropical forest soils. Ecosphere 6:1–14. doi: 10.1890/ES14-00309.1

588 Liptzin D, Silver WL, Detto M (2011) Temporal dynamics in soil oxygen and greenhouse gases
589 in two humid tropical forests. Ecosystems 14:171–182. doi: 10.1007/s10021-010-9402-x

590 Lovley DR (1995) Microbial reduction of iron, manganese, and other metals. Adv Agron
591 54:175–231.

592 Melton ED, Swanner ED, Behrens S, et al (2014) The interplay of microbially mediated and
593 abiotic reactions in the biogeochemical Fe cycle. Nat Rev Microbiol 12:797–808. doi:
594 10.1038/nrmicro3347

595 Nepstad DC, de Carvalho CR, Davidson EA, et al (1994) The role of deep roots in the
596 hydrological and carbon cycles of Amazonian forests and pastures. Nature 372:666–669.
597 doi: 10.1038/372666a0

598 Norkko J, Reed DC, Timmermann K, et al (2011) A welcome can of worms? Hypoxia mitigation
599 by an invasive species. Glob Change Biol 18:422–434. doi: 10.1111/j.1365-
600 2486.2011.02513.x

601 Peretyazhko T, Sposito G (2005) Iron(III) reduction and phosphorous solubilization in humid
602 tropical forest soils. Geochim Cosmochim Acta 69:3643–3652. doi:
603 10.1016/j.gca.2005.03.045

604 Pfennig N, Trüper HG (1992) The family Chromatiaceae. In: Balows A, Trüper HG, Dworkin M,
605 et al. (eds) The Prokaryotes. Springer, New York, USA, pp 3200–3221

606 Ponnamperuma FN (1972) The chemistry of submerged soils. Adv Agron 24:29–96.

607 Raich JW, Schlesinger WH (1992) The global carbon dioxide flux in soil respiration and its
608 relationship to vegetation and climate. Tellus B 44:81–99. doi: 10.1034/j.1600-
609 0889.1992.t01-1-00001.x

610 Roden E, Wetzel R (1996) Organic carbon oxidation and suppression of methane production by
611 microbial Fe(III) oxide reduction in vegetated and unvegetated freshwater wetland
612 sediments. Limnol Oceanogr 41:1733–1748.

613 Roden EE, Wetzel RG (2002) Kinetics of microbial Fe(III) oxide reduction in freshwater
614 wetland sediments. Limnol Oceanogr 47:198–211.

615 Roden EE, Zachara JM (1996) Microbial reduction of crystalline Iron(III) oxides: influence of
616 oxide surface area and potential for cell growth. Environ Sci Technol 30:1618–1628. doi:
617 10.1021/es9506216

618 Sanchez PA (1976) Properties and Management of Soils in the Tropics. John Wiley and Sons,
619 New York

620 Schulz M, Stonestrom D, Lawrence C, et al (2016) Structured heterogeneity in a marine terrace
621 chronosequence: upland mottling. Vadose Zone J 15:0. doi: 10.2136/vzj2015.07.0102

Schulz MS, White AF (1999) Chemical weathering in a tropical watershed, Luquillo Mountains, Puerto Rico III: quartz dissolution rates. Geochim Cosmochim Acta 63:337–350. doi: 10.1016/S0016-7037(99)00056-3

Schwertmann U, Murad E, others (1988) The nature of an iron oxide-organic iron association in a peaty environment. Clay Miner 23:291–299.

Seitzinger S, Harrison JA, Böhlke JK, et al (2006) Denitrification across landscapes and waterscapes: a synthesis. Ecol Appl 16:2064–2090. doi: 10.1890/1051-0761(2006)016[2064:DALAWA]2.0.CO;2

Sexstone A, Revsbech N, Parkin T, Tiedje J (1985) Direct measurement of oxygen profiles and denitrification rates in soil aggregates. Soil Sci Soc Am J 49:645–651.

Silver WL, Liptzin D, Almaraz M (2013) Soil redox dynamics and biogeochemistry along a tropical elevation gradient. In: Gonzalez G, Willig MR, Waide RB (eds) Ecological Gradient Analyses in a Tropical Landscape. Wiley, NJ, USA,

Silver WL, Lugo AE, Keller M (1999) Soil oxygen availability and biogeochemistry along rainfall and topographic gradients in upland wet tropical forest soils. Biogeochemistry 44:301–328. doi: 10.1023/A:1006034126698

Soil Survey Staff (2002) Soil survey of Caribbean National Forest and Luquillo Experimental Forest, Commonwealth of Puerto Rico. United States Department of Agriculture, Natural Resources Conservation Service

Solomon DK, Cerling TE (1987) The annual carbon dioxide cycle in a montane soil: Observations, modeling, and implications for weathering. Water Resour Res 23:2257–2265. doi: 10.1029/WR023i012p02257

Stone MM, DeForest JL, Plante AF (2014) Changes in extracellular enzyme activity and microbial community structure with soil depth at the Luquillo Critical Zone Observatory. Soil Biol Biochem 75:237–247. doi: 10.1016/j.soilbio.2014.04.017

Straub KL, Benz M, Schink B, Widdel F (1996) Anaerobic, nitrate-dependent microbial oxidation of ferrous iron. Appl Environ Microbiol 62:1458–1460.

Thamdrup B (2000) Bacterial manganese and iron reduction in aquatic sediments. In: Schink B (ed) Advances in Microbial Ecology. Springer, Boston, MA, pp 41–84

Thompson A, Chadwick OA, Boman S, Chorover J (2006) Colloid mobilization during soil iron redox oscillations. Environ Sci Technol 40:5743–5749. doi: 10.1021/es061203b

Thompson A, Rancourt D, Chadwick O, Chorover J (2011) Iron solid-phase differentiation along a redox gradient in basaltic soils. Geochim Cosmochim Acta 75:119–133. doi: 10.1016/j.gca.2010.10.005

656 Veneman PLM, Vepraskas MJ, Bouma J (1976) The physical significance of soil mottling in a
657 Wisconsin toposequence. Geoderma 15:103–118. doi: 10.1016/0016-7061(76)90081-1

658 Viollier E, Inglett P, Hunter K, et al (2000) The ferrozine method revisited: Fe(II)/Fe(III)
659 determination in natural waters. Appl Geochem 15:785–790. doi: 10.1016/S0883-
660 2927(99)00097-9

661 von Fischer JC, Hedin LO (2007) Controls on soil methane fluxes: Tests of biophysical
662 mechanisms using stable isotope tracers. Glob Biogeochem Cycle 21:9. doi: Gb2007
663 10.1029/2006gb002687

664 Weaver PL, Murphy PG (1990) Forest structure and productivity in Puerto Rico's Luquillo
665 Mountains. Biotropica 22:69–82. doi: 10.2307/2388721

666 Weber KA, Achenbach LA, Coates JD (2006) Microorganisms pumping iron: anaerobic
667 microbial iron oxidation and reduction. Nat Rev Microbiol 4:752–764. doi:
668 10.1038/nrmicro1490

669 White AF, Blum AE, Schulz MS, et al (1998) Chemical weathering in a tropical watershed,
670 Luquillo Mountains, Puerto Rico: I. Long-term versus short-term weathering fluxes.
671 Geochim Cosmochim Acta 62:209–226. doi: 10.1016/S0016-7037(97)00335-9

672 Widdel F, Bak F (1992) Gram-negative mesophilic sulfate-reducing bacteria. In: Balows A,
673 Trüper HG, Dworkin M, et al. (eds) The Prokaryotes. Springer New York, pp 3352–3378

674 Yang WH, Liptzin D (2015) High potential for iron reduction in upland soils. Ecology 96:2015–
675 2020. doi: 10.1890/14-2097.1

676 Yang WH, Weber KA, Silver WL (2012) Nitrogen loss from soil through anaerobic ammonium
677 oxidation coupled to iron reduction. Nat Geosci 5:538–541. doi: 10.1038/ngeo1530

678 Yi-Balan SA, Amundson R, Buss HL (2014) Decoupling of sulfur and nitrogen cycling due to
679 biotic processes in a tropical rainforest. Geochim Cosmochim Acta 142:411–428. doi:
680 10.1016/j.gca.2014.05.049

681

682 **Figure captions:**

683 Figure 1: Idealized depth profiles of bulk O_2 (solid line) and Fe(II) (dashed line) with depth.

684 Panel **a** represents a standard conceptual model for aquatic sediments, where Fe reduction occurs

685 at depths below which O_2 and other oxidants (not shown for clarity) have been reduced. Panel **b**

686 shows an alternative model for terrestrial soils where bulk O_2 decreases slightly with depth, and

687 total Fe reduction peaks in anaerobic microsites near the soil surface as a consequence of greater
688 availability of C and short-range-ordered Fe. Oxygen profiles were modeled after Cerling (1991),
689 assuming a stoichiometric relationship between CO_2 and O_2 and an exponential decline in CO_2
690 production with depth; diffusivity differs for panels **a** and **b**. Iron(II) trends are hypothetical but
691 consistent with previous work at this site; labile Fe(II) may increase near bedrock due to supply
692 from primary minerals (Buss et al. 2005).

693 Figure 2: Soil O_2 concentrations (**a)** measured at hourly intervals along the Guaba ridge depth
694 profile from June 2010 to February 2012. Boxes represent medians and the first and third
695 quartiles. Whiskers represent the furthest value less than 1.5 times the box length measured from
696 the box edge; more extreme points are denoted as circles. Mean (± SE) concentrations of
697 $Fe(II)_{HCl}$ (**b**), $Fe(III)_{HCl}$ (**c**), and soil respiration (**d**) were measured shortly after sampling (n = 3
698 per depth). Means with different letters differed significantly ($p < 0.05$, Tukey comparison).

699 Figure 3: Net Fe(II) production by depth (± SE) over a 10-day incubation of intact (non-slurried)
700 soils under anaerobic conditions (n = 3 per depth). Note that bar widths are not proportional to
701 soil depths (as in Fig. 2) because a subset of depths was measured.

702 Figure 4: Iron reduction during three-day anaerobic incubations of intact (non-slurried) soils
703 from 0 – 0.1 m depth, incubated with varying concentrations of labile C (glucose) and short-
704 range-ordered Fe(III). Treatments with different letters differed significantly (all possible
705 pairwise comparisons were evaluated), and whiskers represent standard errors (n = 3 per
706 treatment).

707 Figure 5: Rates of Fe reduction (**a**) and most-probable-number (MPN) analyses of Fe reducers
708 (**b**) and oxidizers (**c**) measured before and after anaerobic incubations of soil slurries. Samples

were amended with NO_3^-, Fe as ferrous chloride, NO_3^- + Fe, acetate, or acetate + NO_3^-. Means with different letters within a given depth increment differed significantly (n = 4 per treatment).

727 Figure 1:

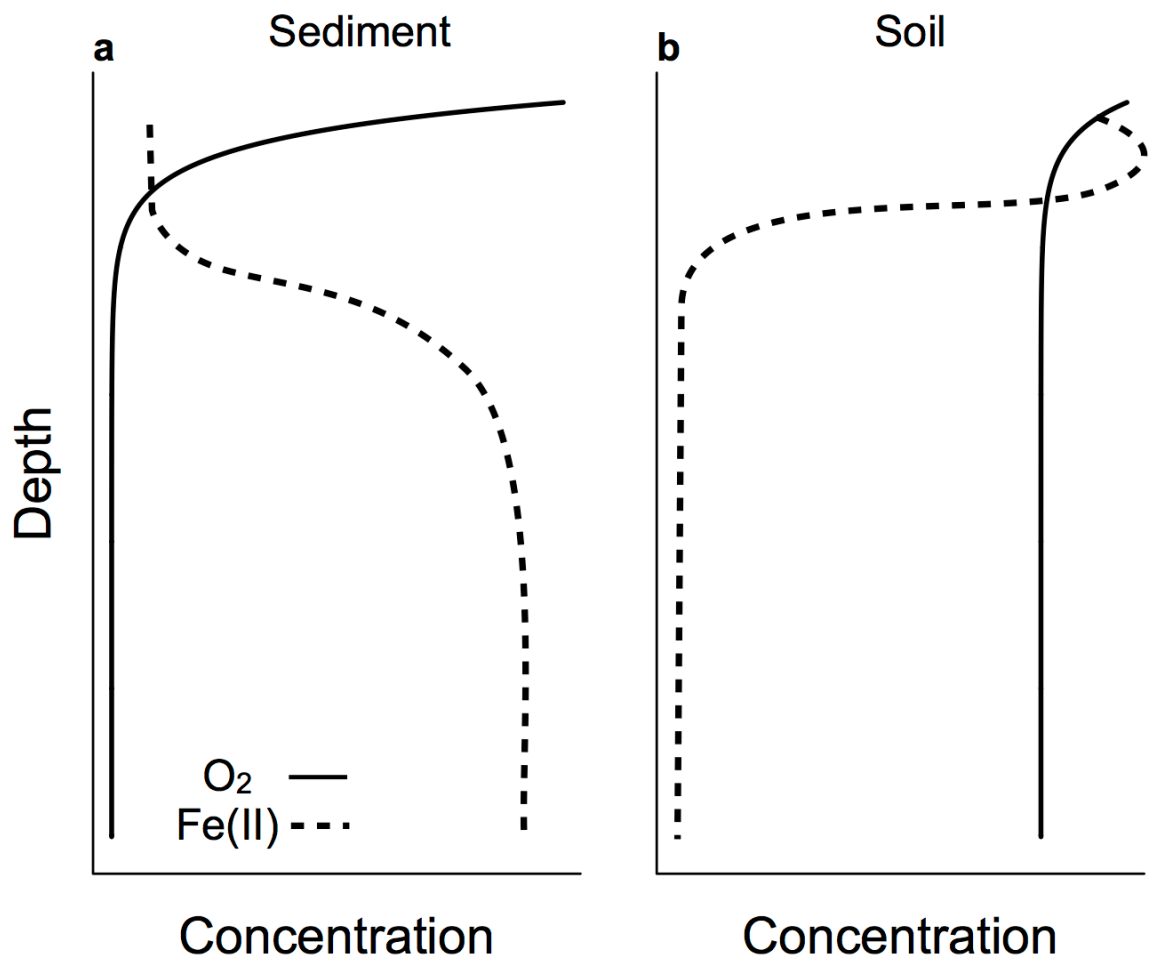

728

729

730

731

732

733

734

735 Figure 2:

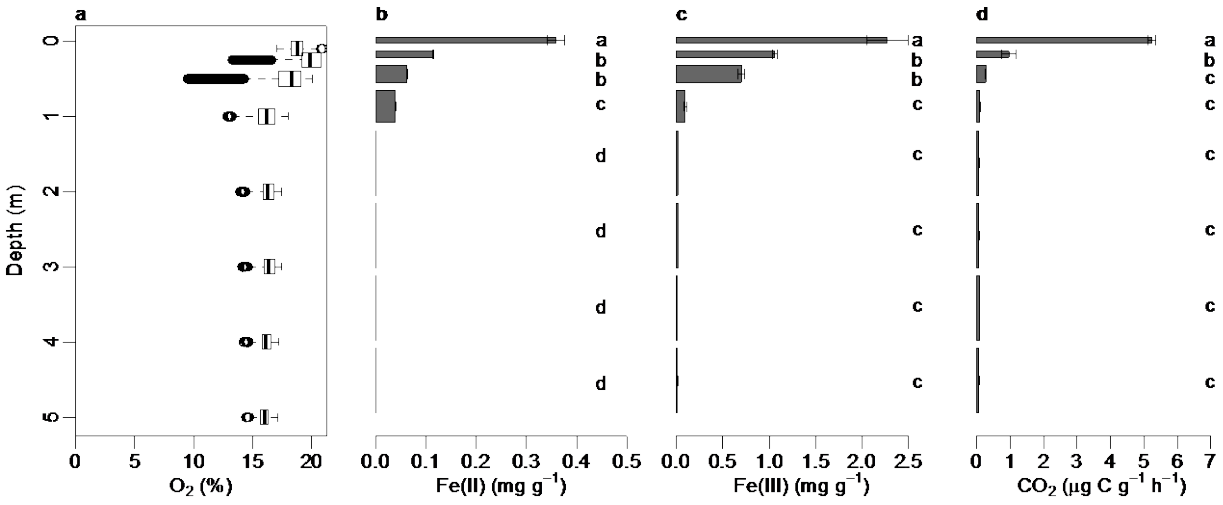

736

737

738

739

740

741

742

743

744

745

746

747

748 Figure 3:

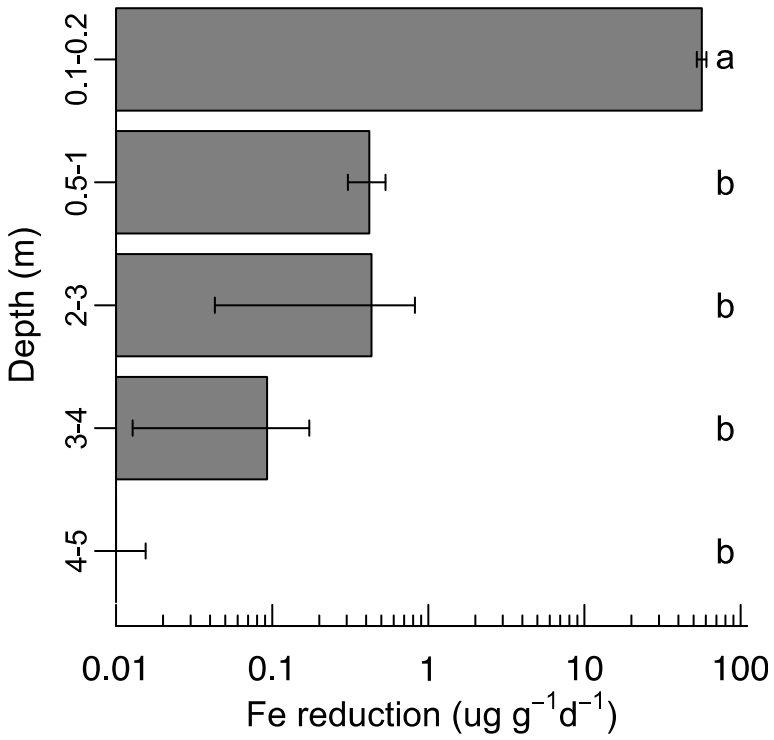

749

750

751

752

753

754

755

756

757

Figure 4:

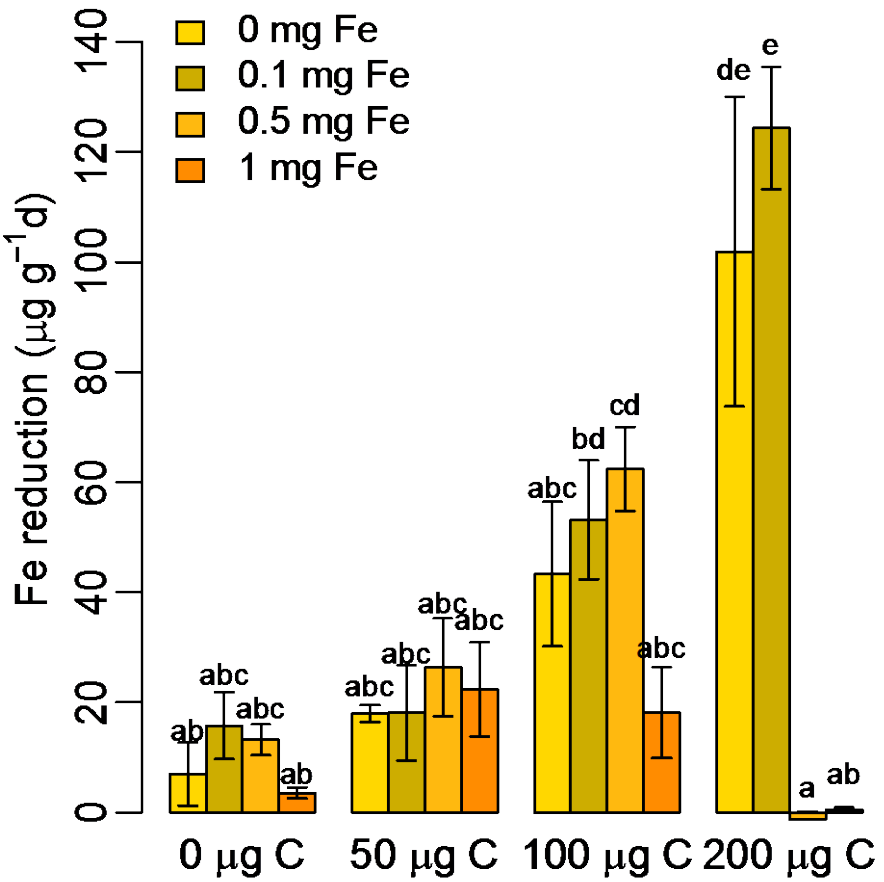
0 mg Fe
0.1 mg Fe
0.5 mg Fe
1 mg Fe
Fe reduction (µg g^{-1}d)
0
20
40
60
80
100
120
140
ab
abc
abc
ab
abc
abc
abc
abc
abc
bd
cd
abc
de
e
a
ab
0 µg C
50 µg C
100 µg C
200 µg C

767 Figure 5:

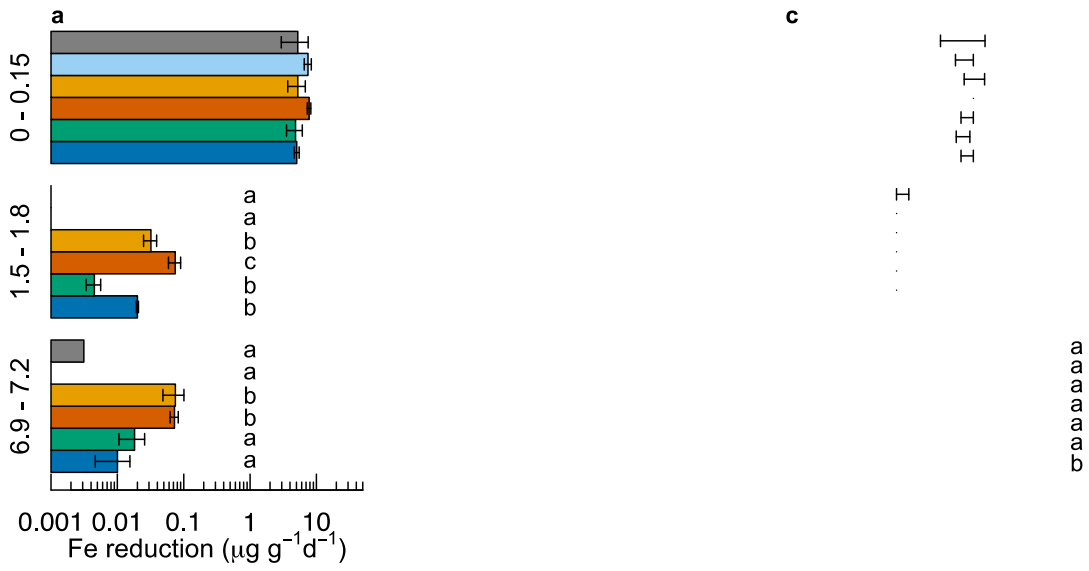

768